insensitive to the ionic strength while a change in ionic strength from 1.0 to 4.0 M resulted in an increase of ~25% in k_{obs} obtained at 1.0 M NaOH.

REFERENCES

(1) V. Stella and T. Higuchi, *J. Pharm. Sci.*, **62**, 968 (1973) and reference therein.

(2) E. Friedmann, D. H. Marrian, and I. Simon-Reuss, *Br. J. Pharmacol.*, **4**, 105 (1949); *Biochim. Biophys. Acta*, **9**, 61 (1952); E. Friedmann, *Bull. Soc. Chim. Biol.*, **31**, 506 (1949).

(3) T.-C. Tsao and K. Bailey, *Biochim. Biophys. Acta*, **11**, 102 (1953).

(4) C. O'Connor, *Quart. Rev. Chem. Soc.*, **24**, 553 (1970); M. L. Bender, *Chem. Rev.*, **60**, 53 (1960).

(5) S. S. Biechler and R. W. Taft, *J. Am. Chem. Soc.*, **79**, 4927 (1957).

(6) M. Komiyama and M. L. Bender, *Bioorg. Chem.*, **7**, 133 (1978); R. M. Pollack and T. C. Dumsha, *J. Am. Chem. Soc.*, **97**, 377 (1975); F. Kezdy and A. Bruylants, *Bull. Soc. Chim. Belg.*, **69**, 602 (1960); F. M. Menger and J. A. Donohue, *J. Am. Chem. Soc.*, **95**, 432 (1973); E. G. Sander, *J. Am. Chem. Soc.*, **91**, 3629 (1969); M. N. Khan and A. A. Khan, *Indian J. Chem.*, **13**, 485 (1975).

(7) M. N. Khan and T. O. Olagbemiro, *J. Org. Chem.*, **47**, 3695 (1982).

(8) M. N. Khan, R. Ahmad, and A. A. Khan, *Indian J. Chem.*, **14A**, 961 (1976); R. Ahmad, M. N. Khan, and A. A. Khan, *Indian J. Chem.*, **14A**, 807 (1976); M. N. Khan and A. A. Khan, *J. Chem. Soc., Perkin Trans. 2*, **1978**, 1176.

(9) M. N. Khan and A. A. Khan, *J. Chem. Soc., Perkin Trans. 2*, 796, 1093 (1979); *J. Chem. Soc., Perkin Trans. 2*, **1976**, 1009; *Indian J. Chem.*, **21A**, 365 (1982).

(10) R. J. E. Talbot, in "Comprehensive Chemical Kinetics," vol. 10, C. H. Bamford and C. F. H. Tipper, Eds., Elsevier, Amsterdam, The Netherlands, 1972, pp. 274, 275.

(11) M. N. Khan, *J. Org. Chem.*, **48**, 2046 (1983).

(12) G. Dahlgren and N. L. Simmerman, *J. Phys. Chem.*, **69**, 3626 (1965).

(13) R. Kluger and J. Chin, *J. Am. Chem. Soc.*, **104**, 2891 (1982); A. J. Kirby and P. W. Lancaster, *J. Chem. Soc. Perkin Trans. 2*, **1972**; 1206.

(14) M. F. Aldersley, A. J. Kirby, P. W. Lancaster, R. S. McDonald, and C. R. Smith, *J. Chem. Soc., Perkin Trans. 2*, **1974**, 1487.

(15) M. N. Khan and L. Malspeis, *J. Org. Chem.*, **47**, 2731 (1982).

(16) A. A. Frost and R. G. Pearson, "Kinetics and Mechanism," Wiley-Interscience, New York, N.Y., 1961, chap. 7.

(17) E. Grunwald and S. Winstein, *J. Am. Chem. Soc.*, **70**, 846 (1948).

(18) A. H. Fainberg and S. Winstein, *J. Am. Chem. Soc.*, **78**, 2770 (1956).

(19) M. J. Gresser and W. P. Jencks, *J. Am. Chem. Soc.*, **99**, 6963 (1977); 6970 (1977); D. J. Hupe and W. P. Jencks, *J. Am. Chem. Soc.*, **99**, 451 (1977).

(20) (a) G. B. Barlin and D. D. Perrin, *Quart. Rev. Chem. Soc.*, **20**, 75 (1966). (b) I. T. Ibrahim and A. Williams, *J. Chem. Soc. Perkin Trans. 2*, **1982**, 1459.

(21) C. D. Ritchie, D. J. Wright, D-S. Huang, and A. A. Kamego, *J. Am. Chem. Soc.*, **97**, 1163 (1975).

(22) M. N. Khan and A. A. Khan, *J. Org. Chem.*, **40**, 1793 (1975).

(23) G. J. Yakatan and T. Fun, *Drug Dev. Ind. Pharm.*, **3**, 315 (1977).

(24) W. P. Jencks, *Accounts Chem. Res.*, **13**, 161 (1980).

(25) N. Gravitz and W. P. Jencks, *J. Am. Chem. Soc.*, **96**, 489, 499, 507 (1974).

(26) E. Grunwald, C. F. Jumper, and S. Meiboom, *J. Am. Chem. Soc.*, **85**, 522 (1963); Z. Luz and S. Meiboom, *J. Am. Chem. Soc.*, **85**, 3923 (1963); S. Rosenberg, S. M. Silver, J. M. Sayer, and W. P. Jencks, *J. Am. Chem. Soc.*, **96**, 7986 (1974); R. Kluger and C.-H. Lam, *J. Am. Chem. Soc.*, **100**, 2191 (1978).

(27) A. Bruylant and F. Kezdy, *Rec. Chem. Progr.*, **21**, 213 (1960); R. H. DeWolfe and R. C. Newcomb, *J. Org. Chem.*, **36**, 3870 (1971).

(28) K. J. Laidler, "Chemical Kinetics," McGraw-Hill, New York, N.Y., 1965.

(29) J. C. Tillett and D. E. Wiggins, *Tetrahedron Lett.*, **14**, 91 (1971).

ACKNOWLEDGMENTS

The author is very grateful to the Research and Higher Degrees Committee of Bayero University for a research grant to purchase the UV-visible spectrophotometer.

Dissolution at Porous Interfaces VI: Multiple Pore Systems

H. GRIJSEELS *, D. J. A. CROMMELIN ˣ, and C. J. DE BLAEY ‡

Received February 3, 1983, from the *Department of Pharmaceutics, University of Utrecht, 3511 GH Utrecht, The Netherlands.* Accepted for publication March 21, 1984. Present addresses: *Gist-brocades N.V., P.O. Box 43, 7940 AA Meppel, The Netherlands and ‡Royal Dutch Society for the Advancement of Pharmacy, 2514 JL The Hague, The Netherlands.

Abstract □ With the aid of rapidly dissolving sodium chloride particles, cubic pores were made in the surface of a theophylline tablet. The influence of the pores on the dissolution rate of the surface was investigated in a rotating disk apparatus. Like the drilled pores used in earlier studies, downstream on the surface they caused a turbulent flow regimen with the development of a trough due to enhanced erosion. The phenomenon of a critical pore diameter, discovered with single, drilled pores, seems to be applicable to the cubic pores investigated in this study, although a higher degree of surface coverage with pores caused complications, probably due to particles bordering one another and forming larger pores. The behavior of the porous surfaces at different rotation speeds was studied. Due to the presence of pores the laminar character of the boundary layer flow changes to turbulent, which induces locally an increased dissolution flux in the wake of a pore.

Keyphrases □ Dissolution rates—pore effects, theophylline □ Pore effects—influence on dissolution rate, theophylline

The promoting effect of pores on the dissolution rate of a tablet surface and the effects of individual pores drilled into a dissolving surface have been reported (1–5). The objective of this study was to investigate the changes in dissolution rate of a solid surface when several pores, which can not be considered to act individually, are present. The hydrodynamic conditions around each pore will be influenced by surrounding pores and, as a consequence of the interaction of the turbulent zones behind the pores, the erosion troughs will overlap.

Pores can be drilled into a tablet surface by a drilling technique (1–5), but this method is not feasible for a large number of pores, and an alternative procedure was followed in this study. Sodium chloride particles, characterized by an almost cubic shape, were embedded in the surface of a theophylline tablet. In the dissolution experiment, the sodium chloride particles rapidly dissolved leaving (cubic) pores in the slowly dissolving theophylline surface. In this way a surface was easily supplied with a large number of pores.

0022-3549/84/1200-1771$01.00/0

EXPERIMENTAL SECTION

Materials—Theophylline monohydrate[1] was used as supplied. Sodium chloride was classified by sieving. Both compounds met the requirements of the European Pharmacopoeia (6).

Particle Size Determinations—The size distribution of the sieve fractions of sodium chloride particles was determined by microscopic examination. As nearly all particles had a cubic shape, the edge of each particle was measured as its characteristic diameter. Cumulative log-probability plots of the particle distribution data gave straight lines, from which the geometric mean diameter (d_g) and the geometric standard deviation (σ_g) of each fraction were obtained. The specific gravity (ρ) of sodium chloride is 2.17×10^3 kg·m^{-3} (7) and since on the whole the shape of the particles is cubic, d_g was used to compute the number of particles per unit weight by:

$$n = \frac{1}{\rho d_g^3} \qquad \text{(Eq. 1)}$$

Disk Preparation—Tablets with a 15.0-mm diameter and varying thicknesses were compressed individually using a hydraulic press. The flat surfaces of each tablet were perfectly smooth without rims or ridges, which was achieved by using an appropriate set of die and punches. After inserting the lower punch in the die, a quantity of theophylline powder, sufficient to obtain a tablet with a thickness of 2–4 mm, was poured into the die. Next, the upper punch was mounted and the powder was precompressed at 2000 N for 10 s. After removing the upper punch, a small amount of sodium chloride was put on the theophylline surface. The particles were carefully spread over the surface to obtain a homogeneous distribution. The actual compression was then performed at 12,000 N for ≥30 s. At this compressional force the sodium chloride crystals did not break or disintegrate (checked microscopically). This procedure provided tablets with an upper surface consisting of intact cubic sodium chloride particles embedded in a theophylline matrix.

Dissolution Rate Measurements—The rotating disk apparatus for determining the dissolution rate of the tablet surfaces has been described in detail (2). In this study the rotation speed of the mounted disk varied between 100 and 340 rpm. The concentrations of sodium chloride and theophylline were measured continuously and simultaneously. The quantity of dissolved sodium chloride was monitored by a conductivity cell[2] mounted in the vessel. The theophylline concentration was measured by circulating the solution through a spectrophotometer[3] equipped with a flow cell (10-mm path length) and set at a wavelength of 270 nm. An internal calibration of both measuring systems was performed by the preaddition method described previously (1).

To be sure that dissolved sodium chloride had no influence on the absorbance of theophylline, increasing amounts of solid sodium chloride were added to a theophylline solution: no change in absorbance was noticed and, conversely, adding solid theophylline to a sodium chloride solution had no effect on the measured conductance. The dissolution rate of a smooth theophylline surface into bulk solutions with different concentrations of sodium chloride was measured and, for the sodium chloride concentrations relevant to this study, the dissolution rate of theophylline was not affected by the amount of sodium chloride in the solution.

After a short initial period, during which the sodium chloride particles dissolved, the theophylline dissolution curves were straight up to ≥15 min. This was sufficient to obtain an accurate value for the dissolution rate. Dissolution data were collected at regular time intervals by a microcomputer[4]. After the experiment, the dissolution rate of the theophylline surface was computed from the least-squares regression line of those data that were obtained after the sodium chloride had dissolved completely, *i.e.*, after the conductance of the solution had reached a constant level (in all cases within 60 s). At that moment only a negligible quantity of theophylline had dissolved (~5–10% of the final amount), implying that the shape of the created pores had hardly changed during this initial period. The conductance of the solution was measured after complete dissolution of the embedded sodium chloride; from this measurement the number of crystals originally present in the surface, which equals the number of created pores, was calculated.

RESULTS AND DISCUSSION

The erosion pattern of a tablet after the dissolution rate experiment (Fig. 1), is the result of two processes. First, dissolution of the sodium chloride particles creates cubic pores. Due to the presence of these pores in the surface troughs develop, which are the consequence of an enhanced theophylline dissolution in the wake of the pores and which extend along a spiral trajectory in the theophylline surface (2).

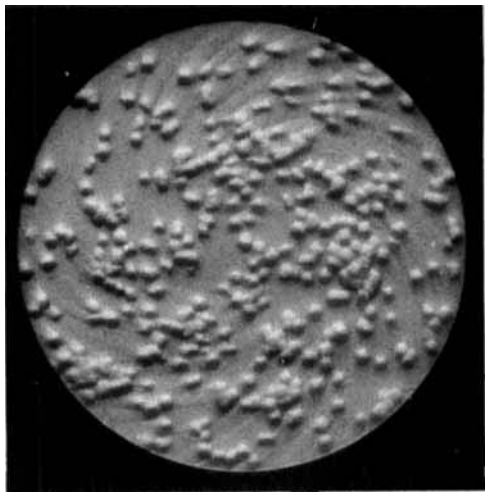

Figure 1—*The surface of a theophylline tablet after a dissolution experiment of ~15 min. Pores were created by sodium chloride particles (d_g = 308 μm), embedded in the surface.*

The dissolution rates of porous theophylline surfaces were determined at a rotation speed of 160 rpm using a varying number of sodium chloride particles of different sizes. Porous surfaces were made with the five sieve fractions listed in Table I. In all experiments the maximum coverage of the theophylline surface by sodium chloride particles remained <25%.

For each sieve fraction the dissolution rate of a theophylline surface with n pores (R_n) was measured at various values of n. In Fig. 2, I_n, the difference between the dissolution rates of a smooth surface (R_0) and a surface with n pores (R_n), is plotted as a function of the number of pores. Since the dissolution rate of a smooth theophylline surface at 160 rpm is 14.9 μg·s^{-1}, the largest pores can cause the dissolution rate to increase >50% at this rotation speed.

Figure 2 demonstrates that I_n is not only dependent on the number of pores but also on the pore size. This is not surprising in view of previous findings (1–5). It was established (3) that the critical pore diameter (the diameter a single pore must exceed to cause an increase of the dissolution rate) is related to the friction velocity v_f in the boundary layer at the rotating disk surface according to:

$$d_{crit} = 2.7 \frac{\nu}{v_f} \qquad \text{(Eq. 2)}$$

where ν is the kinematic viscosity of the solvent (mm^2·s^{-1}).

The friction velocity is a hydrodynamic variable that, for a rotating disk surface, can be computed from (8, 9):

$$v_f = 0.89 \nu^{1/4} x^{1/2} \omega^{3/4} \qquad \text{(Eq. 3)}$$

where x is the distance from the surface center (mm) and ω is the angular velocity (s^{-1}). Equation 3 implies that at the edge of the dissolving surface the friction velocity has a maximum value and, from Eq. 2, the critical pore diameter has a minimum value. With a rotation speed of 160 rpm the critical pore diameter at the edge (calculated from Eqs. 2 and 3) is ~0.13 mm. Nearer the disk center d_{crit} is larger, *e.g.*, at 2.5 mm from the surface edge a value of 0.19 mm was measured (3).

These considerations made it unlikely that the sodium chloride fractions with a d_g of ~ ≤130 μm would cause an increase in the dissolution rate. Even the 198-μm fraction could only increase the dissolution rate on a limited part

Table I—Sieve Fraction Data of Sodium Chloride

Sieve Fraction, μm	Geometric Mean Diameter (d_g), μm	Geometric *SD* (σ_g)	Calculated Particle Number (n)[a]
71–100	88	1.28	676
100–160	128	1.23	220
160–250	198	1.18	59
250–400	308	1.16	15.8
400–500	419	1.15	6.3

[a] Number of particles/mg sodium chloride.

[1] OP6, Utrecht, The Netherlands.
[2] PW9510; Philips.
[3] UV100-02; Shimadzu.
[4] Apple II plus.

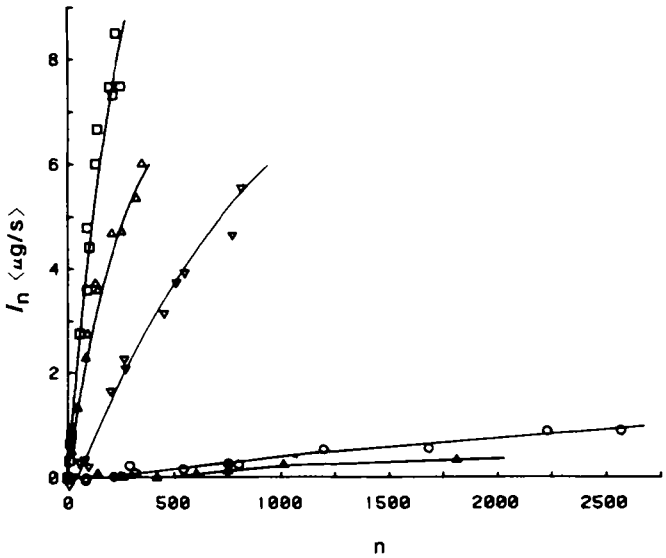

Figure 2—*Effect of number and size of pores on the increase in dissolution rate of the theophylline surface with respect to a smooth surface (160 rpm). Key: particles with a geometric mean diameter of (□) 419 μm; (△) 308 μm; (▽) 198 μm; (○) 128 μm; (▲) 88 μm.*

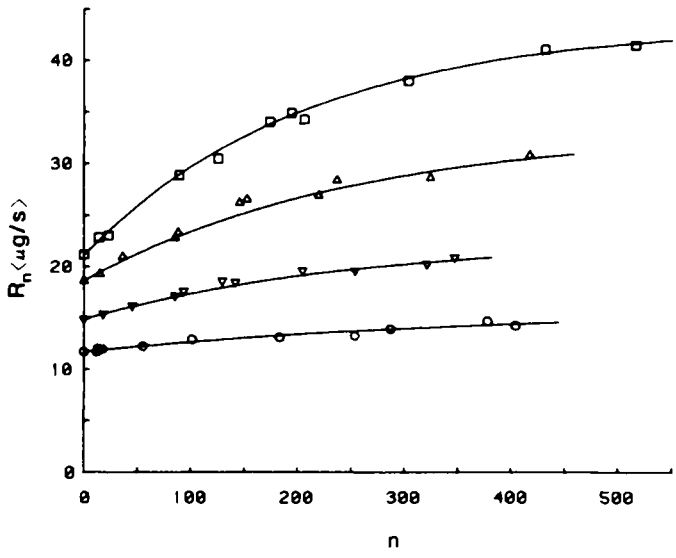

Figure 3—*Dissolution rate of a theophylline surface at different rotation speeds as a function of the number of sodium chloride particles used to create pores. Geometric mean diameter of the particles: 308 μm. Key: (□) 340 rpm; (△) 250 rpm; (▽) 160 rpm; (○) 100 rpm. Each symbol represents an individual experiment. Lines were computed by Eq. 7.*

of the surface; only particles positioned in a region of the tablet surface where d_{crit} is less than ~0.20 mm can cause a change in the dissolution rate. The more particles present in the surface, the more likely it is that somewhere a pore exceeds the local critical size. In the 198-μm fraction, the dissolution rate increases considerably with n, provided that n exceeds a minimum value of 30–40 particles (Fig. 2).

A second possible explanation for the shape of the lines in Fig. 2 must be mentioned. Single particles that create pores equal to or smaller than the local critical size, will not raise the dissolution rate, but when the number of particles in the surface increases, it is more likely that at least two particles lie against each other and together create a larger pore when the sodium chloride dissolves. The presence of these larger pores might be the reason that, at higher values of n, the two smallest particle fractions (128 and 88 μm) also cause a slight increase in the dissolution rate compared with a smooth surface.

The influence of the rotation velocity of the disk surface on the dissolution rate was investigated using the 308-μm particles. The relationship between dissolution rate and number of particles was determined at four different revolution speeds (Fig. 3). No linear relation exists between those two variables, but for every rotation speed the dissolution rate (R_n) increases asymptotically with increasing n to a maximum value. This leads to the assumption that for a certain number of pores a maximum dissolution rate (R_{max}) exists. The corresponding maximum increase of the dissolution rate, I_{max}, is defined by:

$$I_{max} = R_{max} - R_0 \qquad \text{(Eq. 4)}$$

Suppose that the relation between I_n and n can be described by the first-order equation:

$$\frac{d(I_{max} - I_n)}{dn} = -k(I_{max} - I_n) \qquad \text{(Eq. 5)}$$

then we obtain by rearranging and integrating:

$$\ln\left(1 - \frac{I_n}{I_{max}}\right) = -kn \qquad \text{(Eq. 6)}$$

A semilogarithmic plot of $(1 - I_n/I_{max})$ *versus* n should result in a straight line with a slope $-k$ and passing through the origin, provided that the assumption of a first-order relationship in Eq. 5 is justified. Since the value of I_{max} in Eq. 5 was unknown, an iterative calculation of the linear regression coefficients of the data $\ln(1 - I_n/I_{max})$ *versus* n was performed. New values for I_{max} were chosen until the best correlation coefficient was obtained. The computed coefficients were used to fit the data in Fig. 3 according to:

$$R_n = R_0 + I_n = R_0 + I_{max}(1 - e^{-kn}) \qquad \text{(Eq. 7)}$$

The points in Fig. 3 are fitted well by the lines obtained from these computations, so the assumption of a first-order relation appears to be a good approximation.

Table II—Dissolution Rates[a] of Theophylline Surfaces With Cubic Pores

Pores	Rotation Speed, rpm (ω) 100 (10.47)	160 (16.76)	250 (26.78)	340 (35.60)	p[b]	r[c]
0	11.74	14.91	18.60	21.15	0.49	0.9993
10	11.85	15.20	19.18	22.20	0.51	0.9998
20	11.95	15.49	19.73	23.19	0.54	1.0000
30	12.06	15.76	20.26	24.15	0.57	1.0000
40	12.16	16.02	20.77	25.05	0.59	1.0000
50	12.25	16.27	21.26	25.92	0.61	0.9999
75	12.49	16.86	22.41	27.90	0.65	0.9997
100	12.70	17.39	23.44	29.67	0.69	0.9996
125	12.91	17.88	24.38	31.23	0.72	0.9995
150	13.10	18.32	25.22	32.62	0.74	0.9994
200	13.44	19.08	26.68	34.95	0.78	0.9994
250	13.74	19.72	27.87	36.78	0.80	0.9994
300	14.00	20.24	28.84	38.22	0.82	0.9995
350	14.23	20.67	29.63	39.35	0.83	0.9995
400	14.44	21.02	30.28	40.25	0.83	0.9995

[a] Calculated by means of Eq. 7 with the coefficients of the best fit through the experimental data. Pore size, 308 μm. [b] Exponent in Eq. 8, slope, computed from a log-log plot. [c] Correlation coefficient of the log-log plot.

The actual nature of the hydrodynamic conditions at the tablet surface can be determined from the relationship between the dissolution rate and the angular velocity of the rough pellet surface. The relationship between R_n and angular velocity (ω) can be written in the form (10):

$$R_n \sim \omega^p \qquad \text{(Eq. 8)}$$

At smooth rotating disk surfaces, p = 0.5 under laminar conditions and p = 0.9 in a completely turbulent flow pattern. At a rough rotating disk surface, consisting of a regular, geometric pattern of pyramids, the following results were obtained (11-14): with a pyramid height of >1 mm the mass flux varied with $\omega^{0.67}$. But when the height of the roughness elements diminished, the exponent of ω increased from 0.67 to >0.9 (14). The experimental data collected in Fig. 3 were used to investigate the effect of the presence of pores on the hydrodynamics at the tablet surface. Since the dissolution rates can be compared only for equal values of n at the different rotation speeds, interpolated values of R_n were calculated by Eq. 7 from the best fit of the experimental data for various numbers of pores at each rotation speed (Table II). A linear regression analysis of the plot of log R_n *versus* log ω for any number of pores was performed on the data collected in Table II. The slopes of these plots correspond to p in Eq. 8. Exponent p increases from ~0.5 at $n = 0$ (smooth surface) to 0.8-0.9 for surfaces with >250 pores. This confirms earlier observations that, due to the presence of pores, the flow regimen in the boundary layer near the surface shows a transition from laminar to turbulent, resulting in a changed dissolution mechanism of the surface.

REFERENCES

(1) H. Grijseels and C. J. de Blaey, *Int. J. Pharm.*, **9**, 337 (1981).

(2) H. Grijseels, L. van Bloois, D. J. A. Crommelin, and C. J. de Blaey, *Int. J. Pharm.*, **14**, 299 (1983).

(3) H. Grijseels, D. J. A. Crommelin, and C. J. de Blaey, *Int. J. Pharm.* **14**, 313 (1983).

(4) H. Grijseels, B. T. J. M. Harden, and C. J. de Blaey, *Pharm. Weekbl.* **5**, 88 (1983).

(5) H. Grijseels and C. J. de Blaey, *Int. J. Pharm.*, **16**, 295 (1983).

(6) "European Pharmacopoeia," 1st ed., Maisonneuve S.A., Sainte-Ruffine, France, Vol. I, 1969, p. 331; vol. II, 1971, p. 384.

(7) "The Merck Index," 9th ed., Merck & Co., Inc., Rahway, N.J., 1976, p. 1111.

(8) H. Schlichting, "Boundary Layer Theory," McGraw-Hill, New York, N.Y., 1968, pp. 94 and 511.

(9) C. Deslouis, B. Tribollet, and L. Viet, *Electrochim. Acta*, **25**, 1027 (1980).

(10) V. G. Levich, "Physicochemical Hydrodynamics," Prentice Hall, N.J., 1962, pp. 70 and 152.

(11) M. Meklati, M. Daguenet, and G. Cognet, *C. R. Acad. Sci., Paris*, **274**, 1373 (1972).

(12) M. Meklati and M. Daguenet, *J. Chim. Phys.*, **70**, 1102 (1973).

(13) M. Meklati and M. Daguenet, *J. Chim. Phys.*, **72**, 262 (1975).

(14) L. Mollet and M. Daguenet, *J. Chim. Phys.*, **78**, 61 (1981).

Interaction of Povidone with Aromatic Compounds V: Relationship of Binding Tendency in a Macromolecular Solution Treated as a Pseudo Two Phase and a Monophase

J. A. PLAIZIER-VERCAMMEN

Received November 12, 1982, from the *Faculteit Geneeskunde en Farmacie, Vrije Universiteit Brussel, B-1090 Brussels, Belgium.* Accepted for publication April 13, 1984.

Abstract □ The pseudo-two-phase model is proposed to correlate complex formation of ligand molecules with povidone with partition coefficients (log P or II constants). The conditions which permit the use of the pseudo-two-phase model for binding of ligand onto macromolecules are determined. This model seems to be a more rational choice than the frequently used complex formation model (monophase). This is demonstrated theoretically and confirmed experimentally. The advantages of the use of such a model are also discussed.

Keyphrases □ Povidone—interaction with aromatic compounds, pseudo-two-phase and monophase systems, salicylic acid, complex formation □ Pseudo-two-phase model—compared with monophase, complex formation aromatic compounds with macromolecules

The important role of lipophilicity of ligand molecules and hydrophobic bonding in complex formation of a series of ligand molecules with povidone has been previously investigated; ligand molecules in the nonionic state showed a higher complexing tendency than those in the ionic state, (1-3). Complex formation of ligand molecules with povidone was explained in terms of hydrophobic bonding (1, 4-8). In earlier work, we studied the complexing tendency of ligand molecules in the nonionic and ionic state, and the importance of the hydrophobic bonding especially for nondissociated molecules was confirmed (9). The correlation observed between the solubility of the ligand molecule in solvent mixtures and its binding to povidone (10) also provided support for the occurrence of complex formation by hydrophobic interactions.

Hansch *et al.* (11) showed that complex formation by hydrophobic bonding of neutral organic molecules with macromolecules, such as serum albumin, can often be correlated with partition coefficients (log P or π constants) (12, 13) between 1-octanol and water. This correlation was found for phenols and serum albumin, barbiturates and homogenized rabbit brain (14), penicillin and serum albumin (15), aniline derivatives and nylon and rayon (16), and phenols and mitochondrial protein (17).

These results, correlated with octanol-water partition coefficients (log P), are expressed either as $1/C$ (11) (where C represents the molar concentration of ligand to produce a one-to-one complex of ligand and macromolecule), as log $B\%$ [percent bound ligand (14)], or as log B/F (15), where B refers to bound and F to free ligand concentrations, respectively. The methods for expressing complex formation are not comparable. As indicated by Bird and Marshall (15), B/F is a more rational choice than $B\%$ for correlating the results with log P, because B/F is analogous to an organic solvent-water partition coefficient. Moreover, as opposed to the other expressions, B is not a linear function of the association constants.

However, the use of the B/F expression has a disadvantage; one must work at a constant macromolecular concentration in order to compare the B/F expressions for the individual ligand molecules with the log P or π values. This implies that one must expect errors in the results obtained for ligand mol-

0022-3549/84/1200-1774$01.00/0